Coupling of the liquid sampling – atmospheric pressure glow discharge (LS-APGD) ionization source with a commercial triple-quadrupole mass spectrometer

Journal:	*Journal of Analytical Atomic Spectrometry*
Manuscript ID	JA-ART-03-2019-000087.R1
Article Type:	Paper
Date Submitted by the Author:	18-Apr-2019
Complete List of Authors:	Williams, Tyler; Clemson University, Chemistry Marcus, R.; Clemson University, Chemistry

Graphical Abstract:

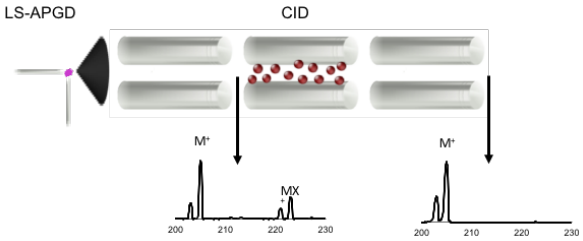

Use of a standard triple-quadrupole mass spectrometer allows for fundamental studies of diverse ion species produced in the LS-APGD microplasma.

Coupling of the liquid sampling – atmospheric pressure glow discharge (LS-APGD) ionization source with a commercial triple-quadrupole mass spectrometer

Tyler J. Williams and R. Kenneth Marcus*

Clemson University, Department of Chemistry, Clemson, SC 29634

*Author to whom correspondence should be addressed

Submitted for publication in the Journal of Analytical Atomic Spectrometry

Abstract

While the LS-APGD microplasma has shown potential as an ionization source for elemental/isotopic/molecular species analysis, up to this point it has been used almost exclusively in conjunction with trapping-type mass analyzers. To this end, the LS-APGD has been coupled to a standard ThermoScientific TSQ Quantum Access MAX triple quadrupole mass spectrometer. This instrument is capable of affecting numerous MS/MS techniques as well as scanning for low mass elements which are not typically permitted in trapping-type MS instruments. The TSQ differs appreciably in how it may be implemented in tandem mass spectrometry versus the triple quadrupoles becoming common in ICP-MS. For example, fragmentation methods such as collision-induced dissociation (CID) in Q2 and in-source CID reduce background spectral contributions can be affected to remediate molecular interferences. With this new coupling, a thorough multi-parametric evaluation was necessary. This evaluation was performed by optimizing the analyte responses and signal-to-background ratios for Rb, Ag, Tl, and U as test elements. With the optimized conditions set, parent ion, product ion, and neutral loss scan methods were explored to observe the types of species being formed by the LS-APGD. While the primary impetus for using the triple quadrupole analyzer was to allow for detailed fundamental studies, LODs for the test elements were determined simultaneously, ranging from 0.99 to 38 ng mL^{-1} for 50 µL injections (i.e., 0.05 – 2 ng absolute mass).

Introduction

Inductively-coupled plasma mass spectrometry (ICP-MS) is a widely used method and arguably among the most powerful methods for elemental analysis. Introduced commercially in 1983, ICP-MS gained quick acceptance due to its incredible sensitivity, robustness, and ability to determine elements in various matrices.[1, 2] While having numerous benefits, ICP-MS suffers from relatively high instrument cost and high consumable use. Spectral interferences had been among the notable drawbacks of this method, leading to a variety of methodologies being developed, including cool plasma conditions and high-resolution sector-field ICP-MS to overcome this issue.[3-5] The most prominent developments for overcoming spectral interferences was the introduction of collision-reaction cells (CRC) used in conjunction with quadrupole mass analyzers to alleviate spectral interferences through chemical reactions to "shift" their masses or through charge neutralization to eliminate the interfering ions.[6-11]

The first commercial iteration of these systems introduced a collision-reaction cell (CRC) followed by the mass-resolving quadrupole mass filter, as first suggested by Rowan and Houk.[12] This cell allows for many spectral interferences to be circumvented through the control of the gas phase reactions taking place. It is important to note that such reactions were thermodynamically driven and not due to kinematics, as is common in organic/molecular mass spectrometry/mass spectrometry (MS/MS).[13, 14] Unfortunately, with no mass-resolving quadrupole located before the CRC, there is no control over the identity of the reactants entering the cells, leading to progeny ions that potentially formed new spectral interferences.[11] After nearly 20 years of prominence, the CRC-quadrupole arrangement is challenged with the introduction of the ICP triple

quadrupole mass spectrometer (QqQ), containing a mass-selective quadrupole mass filter prior to the CRC.[11, 15-17] This allows a specific mass (or range) of ions to be introduced to the CRC, providing increased control over the reactions and collisions that occur. Some of the major interferents this has helped overcome include both argide and doubly charged species. Argide species such as Ar_2^+ are interferents for Se, but by use of a reaction cell with O_2 as the reagent, Se can be measured as SeO^+ with no interferences. Additionally, the formation of doubly charged analyte ions such as Yb^{++} can be interferents for other analytes such as Sr, which can again be overcome using an O_2 reaction gas to measure SrO^+.[11] This configuration has been largely successful in the task of further reducing spectral interferences that plague ICP-MS.

While the ICP-QqQ instruments are effective for reducing interferences, the cost associated with their operation is still appreciable. Beyond initial capital costs, ICP-MS instruments (in general) require 15-20 L min^{-1} of Ar gas to maintain the plasma, plus additional specialty gases for the CRC. In addition to large gas flow rates and high power requirements, solution sample introduction rates up to 0.4 mL min^{-1} make large sample volumes (and coincident waste management) a necessity.[18] These requirements result in ICP-MS instruments which are unsuitable for applications such as field deployment or industrial situations such as at-line biopharmaceutical production environments where size, operational overhead, and simplicity are at a premium. To this end, miniaturized instrumentation (ionization sources and mass analyzers) have been of continued interest.[19]

An important current focus in atomic spectrometry is the development of miniaturized plasmas having low power consumption, low capital cost, and potentially

lower consumable use. Numerous reviews detail the promising results of these devices as they apply to optical emission spectroscopy (OES).[20-22] One particular family of devices was first introduced by Cserfalvi et al. as the electrolyte cathode discharge (ELCAD), developed towards the elemental analysis of water and waste water samples.[23-25] These designs utilize a flowing electrolytic solution to which a plasma is generated. Since this introduction, a number of other studies have improved upon this design, notably the solution cathode glow discharge developed by Hieftje et al.[26] The liquid sampling – atmospheric pressure glow discharge (LS-APGD) developed by Marcus et al., is another source of related design and has been found to have many attractive features.[27] Originally implemented as an OES source,[28] MS sampling has borne out a number of positive attributes towards applications in elemental, isotopic, and molecular species analysis.[29-33] Of particular relevance regarding reduced-overhead elemental MS, the LS-APGD has been shown to run in a total sample consumption mode, with solution and He gas flow rates of <40 μL min^{-1} and <1 L min^{-1}, respectively. Operation with d.c. powers of less than 50 W versus the 1 – 2 kW of rf power for the ICP is a substantial difference as well. The significantly lower operation and consumable costs, and lower power for the LS-APGD make it a promising candidate for those situations not conducive to the use of ICP-MS instruments.

To date, the LS-APGD has been almost exclusively coupled to trapping-type mass spectrometers.[30, 33-37] These couplings have shown promising results in elemental and isotope ratio analysis with LODs in the low ng mL^{-1} to pg mL^{-1} range and providing uranium isotope ratios that meet all applicable IAEA international target values.[33, 35, 36] However, the use of these trapping-type instruments is atypical for elemental analysis,

which rely on quadrupole or sector field instruments. Very recently, this laboratory has described initial efforts in coupling the microplasma to a reduced-format single-quadrupole instrument.[38] While the array of MS platforms has been diverse, many fundamental questions exist as to the chemical species which exist in the plasma. For this reason, a commercial 'organic' triple quadrupole mass spectrometer is utilized here as a means of affecting many diverse MS modalities. While not pertinent in terms of cost or complexity issues regarding miniaturization, the numerous scan modes available to triple-quadrupole instruments as applied in liquid chromatography detection could provide deeper insights into what types of species are being formed within the plasma. Additionally, diverse methods for the reduction of spectral interferences can be investigated to perhaps yield improved analytical figures of merit.

Presented here is the coupling of the LS-APGD with a standard ThermoScientific TSQ Quantum Access MAX triple-quadrupole mass spectrometer. This instrument typically employs electrospray (ESI) or atmospheric pressure chemical ionization (APCI) sources coupled with liquid chromatography for separation and analysis of organic species such as proteins or environmental species. To be clear, the driving force for this particular coupling is the development of a highly versatile tool to study plasma fundamentals. A thorough multi-analyte, parametric evaluation was performed employing a design of experiment (DOE) approach to optimize both signal intensity and signal-to-background ratios (S/B). The included plasma/sampling parameters were discharge current, liquid (sample) flow rate, sheath gas flow rate, distance between the sampling cone and the plasma, and interelectrode gap. Since the LS-APGD has been found to produce oxides, hydroxides, and water clusters, the various MS/MS modes;

precursor ion, product ion, and neutral loss scans, were investigated. At the optimized source conditions, the influence of in-source collision-induced dissociation (CID) voltage, Q2 gas pressure (Ar), and CID energy were evaluated for the purpose of reducing the prevalence of these species and improving S/B ratios. Additionally, LODs were determined simultaneously for a Rb, Ag, Tl, and U multi-element solution. It is believed that while this pairing does not yet yield the same levels of sensitivity seen in couplings with Orbitrap mass spectrometers, it will yield a wealth of qualitative information relevant to improved LS-APGD operation in the future.

Experimental

Source Design

The design of the LS-APGD for interfacing with a mass spectrometer has been previously described.[37] As depicted in Fig. 1, the cathode consists of a fused silica capillary (280 µm i.d., 580 µm o.d., Restek Corporation, Bellefonte, PA) through which an electrolytic solution (sample) is introduced to the plasma (10-80 µL min^{-1}) via a syringe pump (Chemyx Fusion 100, Chemyx, Stafford, TX). The fused silica capillary is housed within an electrically grounded stainless-steel capillary (316 SS, 0.8 mm i.d., 1.6 mm o.d., IDEX Health and Science, Oak Harbor, WA) through which a He sheath gas flows (0.2-0.3 L min^{-1}). The anode is composed of a solid metal electrode (SS, weldable feedthrough; MDC vacuum products, LLC, Hayward, CA, USA) which has a positive potential applied via a Spellman SP60 power supply (0-60 mA, 0-1 kV; Spellman, Hauppauge, NY). The solution cathode is placed in line with the sampling cone (0.5 - 4 mm separation) of the mass spectrometer with the anode being displaced perpendicularly (0.5 – 2 mm), forming the discharge between them.

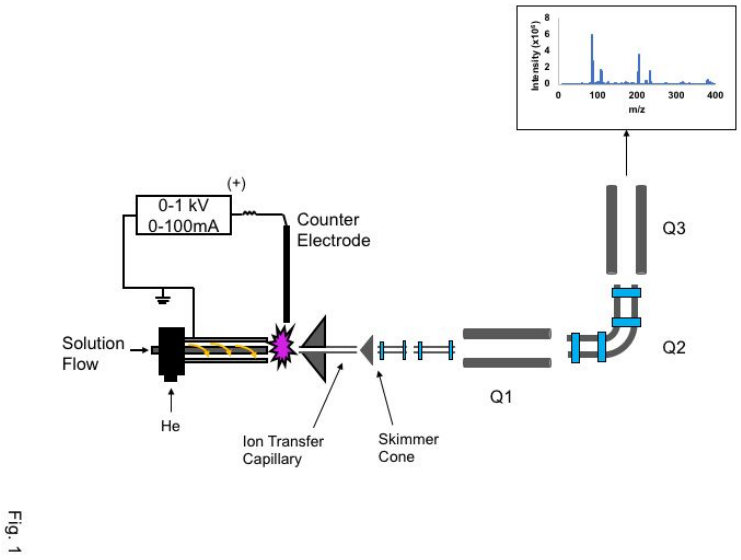

Fig. 1

Figure 1. Diagrammatic representation of the system components of the LS-APGD coupled with the TSQ Quantum Access MAX mass spectrometer.

Mass Spectrometer System

In this work, the LS-APGD was interfaced with a ThermoScientific (San Jose, CA) TSQ Quantum Access MAX triple-quadrupole mass spectrometer requiring no modification to the instrument other than removing the equipped ESI source and mounting the LS-APGD platform. As depicted in Fig. 1, the TSQ system is comprised of the ion sampling capillary and ion optics, the triple quadrupole analyzer, and an electron multiplier detector with a conversion dynode. Different from ICP-QqQ platforms, the second quadrupole in this system is a bent quadrupole into which a collision gas (Ar) can be introduced to affect collisional dissociation (CID). This allows for the ability to perform many different MS/MS operations including parent ion scans, product ion scans, and neutral loss scans.[14] In addition, loosely bound species (usually solvated ions) can be dissociated using the in-source collision induced dissociation by applying a voltage (CID = 0 – 200 V) between the end of the ion transfer capillary and the skimmer

cone. These system parameters are controlled utilizing the Thermo Xcalibur and TSQ Tune Master software systems. Data collected in a full scan mode, or in MS/MS experiments were obtained using a scan rate of 0.5 s across the mass range. In addition, these spectra were collected using the Tune Master software spectrum averaging function, which averages a user-defined number of scans, in this case 10, so that each resulting data point/spectrum is an average of 10 scans. For data collected in the selected ion monitoring (SIM) mode, a scan rate of 0.1 seconds per peak was used as well as the spectrum averaging of 10 scans. In the cases involving ion source optimization and quantitative analysis, Q1 was employed as the mass analyzer while Q2 and Q3 were operated in rf-only modes, serving simply as ion guides.

Design of Experiment

The evaluation of the LS-APGD operating parameters was accomplished by designing an experimental plan using JMP software (SAS Institute Inc., Cary, NC). An initial screening study was carried out in order to rule out non-viable conditions, followed by a custom design experiment was selected and set to find points at which the signal (S) and signal-to-background ratio (S/B) were maximized. Three replicates per condition were randomly placed, resulting in a total of 36 sets of parameters. A 10 μg mL^{-1} multi-element solution was injected (50 μL) at each set of conditions and the analyte ions were determined using selected ion monitoring (SIM). The analyte peak area for each injection was measured, and the S/B was determined using the analyte peak area and the time-equivalent peak area present directly prior to the injection.

This type of parameterization methodology allows for a thorough evaluation without overlooking inter-parametric effects. The resulting plots from these experiments

are shown as bar graphs where the vertical line represents the level of significance. Bars that extend beyond this line indicate a significant influence on the responses, while those that do not, represent an insignificant effect on the targeted responses (S or S/B).[39]

Sample Preparation

A stock multi-element solution covering a broad mass range and different analyte chemistries was prepared from elemental standards (Rb, Ag, and U; High Purity Standards, Charleston, SC) or nitrate salts (Tl; Beantown Chemical, Hudson, NH). The nitrate salts were dissolved using 2% HNO_3 to prepare a 1000 μg mL^{-1} standard solution. The stock multi-element solution was prepared by diluting the standards in 2% HNO_3 to prepare a 10 μg mL^{-1} solution. The test solutions for the calibration curve were made through serial dilution of the stock solution

Results and Discussion

Parametric Evaluation and Coupling Characteristics of the LS-APGD

Prior to this work, the LS-APGD had been coupled almost exclusively to trapping-type mass spectrometers.[30, 33, 35, 36] Previous couplings to the LCQ and Orbitrap instruments explored the dependencies of the signal intensity, S/B ratio, and isotope ratio accuracy on plasma operation parameters. Relevant conditions include discharge current, solution flow rate, sheath gas flow rate, interelectrode gap, and distance from the ion sampling cone. In addition, MS sampling parameters including in-source CID voltage and higher energy collisional dissociation (HCD) were evaluated.[30, 35] In none of the previous efforts was a DOE approach employed.

Through the variety of MS studies using the LS-APGD, the conditions used have seen significant variation between the different couplings. Initial MS studies by Marcus et al. showed that the ideal conditions included low discharge currents (5-10 mA) and low liquid flow rates (<10 μL min^{-1}). In addition, the sheath gas flow rate was optimized to 0.9 L min^{-1} with a ~1 cm sampling distance.[30, 37] More recent studies using the Exactive Orbitrap platform showed that higher liquid flow rates and discharge currents, and lower sheath gas flow rates gave optimal response relative to the formation of the analyte dioxide cation of uranium (UO_2^+).[35] Due to differences in the ion sampling apparatus from the other instruments, a new source optimization was undertaken.

The parameters discussed above were evaluated via the DOE approach with the test matrix generated using the JMP software. A DOE approach models the response of one or more dependent variables based on changing a number of independent variables. In this case, the independent variables were those listed in Table 1, while the dependent variables monitored were the analyte intensity and signal-to-background ratio (S/B). With a software-designed set of parameters probed, the effects of each parameter, as well as inter-parametric effects can be monitored, and their significance determined. Due to the wide range of parameters that have been investigated in previous work, an initial screening study was performed to remove any outlying conditions relative to TSQ sampling. This initial study was used to rule out parameters which provided poor results or were unable to sustain a plasma. Most significantly, the initial study found that the TSQ instrument is unable to handle He sheath gas flow rates above 0.2 L min^{-1} due to increased pressures that trip a vacuum override, disabling high voltage boards in the instrument. This led to significant narrowing of many of the

parameters as the lower gas flow rates resulted in an inability to sustain a plasma at conditions of higher currents (>40 mA) wherein capillaries melt and lower currents (<30 mA) being unable to maintain a plasma at any reasonable solution flow rate. The ultimate parametric test values are detailed in Table 1.

Table 1: Ranges of DOE-evaluated LS-APGD operating conditions and their optimized values.

Parameter	Conditions Tested	Optimized Conditions
Discharge Current	30 - 40 mA	30 mA
Liquid Flow	5 - 30 µL min^{-1}	25 µL min^{-1}
Electrode Gap	0.5 - 2 mm	1 mm
Distance from Sampling Cone	1 - 4 mm	1.5 mm
Gas flow	-	0.2 L min^{-1}

The parametric evaluation was designed using analyte signal and analyte S/B ratios of Rb, Ag, Tl, and U as target responses with the goal of maximizing both. These analytes were used as they cover a range of ionization potentials and chemistries for masses across the periodic table. Figures 2a and b depict the significance of each parameter on the analyte signal (S) response and S/B, respectively. The dashed vertical line in each graph represents the point at which a parameter has a statistically significant effect. In addition, the inter-parametric effects were evaluated and are denoted with a "*" between the two parameters in the legend. Based on Fig. 2a, a number of parameters are shown to have effects on the analyte intensities, three of which are statistically significant. Most significant overall was the effect of the cathode distance from the

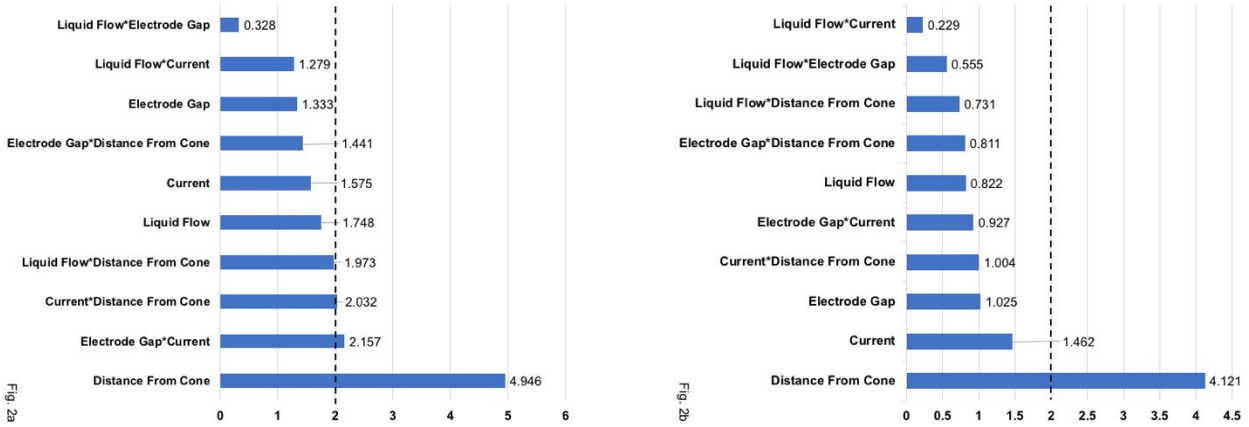

Figure 2. Bar graphs reflecting the combined significance of each operating parameter (and cross effects) on the a) analyte signal intensities (S) and b) analyte signal-to-background ratios (S/B). Analyte concentrations = 10 μg mL^{-1} (each), target analyte isotopes: ^{85}Rb, ^{107}Ag, ^{205}Tl, and $^{238}U^{16}O_2$.

sampling cone, which resulted in a dramatic decrease in analyte intensity at sampling distances greater than 2 mm. This contradicts previous work on the Thermo LCQ which showed an increase in all analyte signal intensity with an increase in the sampling distance.[30] Apart from the sampling distance, a number of inter-parametric effects were observed, the most significant being the cross between the interelectrode gap and discharge current. At 30 mA, the electrode gap has a slightly negative effect on the analyte intensity which is enhanced by the increasing of the current. Different from the other mass analyzers, the TSQ has limited pumping capacity towards helium, limiting the range of sheath gas flow rates. A reduced cooling efficiency at higher currents lead to increased desolvation within the solution capillary and less analyte entering the plasma. While the distance from the sampling cone itself plays a dominant role, its effect is intertwined with both the current and liquid flow rates. It is likely however, that due to the dominating effect the distance from the sampling cone has on the signal

intensity, that these inter-parametric effects are influenced very little by the current and liquid flow rates.

Figure 2b, details the potential influences of the parameters on the S/B ratios, again revealing that the distance from the sampling cone to have the largest influence. In this case, it is the only parameter with a statistically significant effect, showing a decrease in the S/B ratio for all elements as the displacement increased. While this is seen to have a large effect on the signal intensity, with the S/B decreasing with distance it appears to have a less significant effect on the background component. From Fig. 2b, some dependence on the current is also seen, although it is not statistically significant. As seen with previous work, higher currents do lead to increased background species lowering the S/B.[30] Overall, the dependences (or the lack thereof) of the S/B on the various parameters simply reflect the fact that the sources of both S and B are the same. The final optimized conditions for each parameter were determined and are shown in Table 1.

Optimization of In-Source CID Energy and Q2 Gas Pressure

In previous MS couplings of the LS-APGD, the instrument was optimized to reduce interfering ions using in-source CID and the higher-energy collisional dissociation (HCD) cell on Exactive instruments[30, 35] and the CID functionality within the Paul trap of the LCQ.[30] The TSQ, as well, employs a method for in-source CID by applying a potential difference between the ion transfer capillary and the skimmer cone. While no HCD cell is present in this instrument, the argon gas supplied to the Q2 collision cell affects the same processes. To optimize these aspects, 50 µL injections of the 10 µg mL^{-1} multi-element solution were performed, with the resulting S/B ratio for

each analyte computed and used as the test metric. Triplicate injections were performed while varying the in-source CID 0 – 200 V in 25 V increments (with no CID occurring in Q2). After optimization, the same was done for the Q2 gas, varying the pressure from 0 – 5 mTorr at 0.5 mTorr increments.

Previous efforts have shown that in-source CID has a major effect on the levels of background ions related to the aqueous solvent; i.e., ions of the form $M(H_2O)_n^+$ and $(H_2O)_nH^+$. The former species dilute target analyte intensities, while the latter add to spectral background. In principle, increases in energy should better affect dissociation, though the total ion throughput suffers as well with increasing energy. Figure S1 (in Supplementary Information) shows the resulting data from the in-source CID evaluation, suggesting that ~175 V provides the best compromise in S/B for the target analytes. In the case of Rb, Ag, and Tl the loss of background ions generally dominates as the voltage is increased to that point, beyond which the overall transmission begins to suffer. A more interesting scenario is realized in the case of the desired UO_2^+ (m/z = 270 Da) target. The tri-hydrated nitrate form of that ion, $UO_2(NO_3)(H_2O)_3^+$ (m/z = 386 Da) is readily dissociated to the target at very low (<30 eV) potentials, yielding the desired dioxide species. Indeed, the hydrated ion is reduced to near-background levels above 50 eV. The combination of these effects leads to the pronounced improvement in S/B for UO_2^+ at an ITC potential of 175 eV. Overall, operation at that voltage provides levels of background species reductions as seen on previous platforms.

In addition to in-source CID, this instrument offers the ability to induce dissociative collisions in Q2. This involves pressurizing Q2 and applying a potential offset across the quadrupole relative to the exit of Q1. Unfortunately, due to software

limitations, the potential can only be changed during MS/MS scans. Changing this potential would increase the velocity at which the collisions would occur, increasing dissociation. Without this potential, the argon gas pressure in Q2 will still induce dissociation, but to a lesser degree. The effect of the Q2 argon pressure was observed by setting the in-source CID to its optimal point, 175 V, and varying the gas pressure. Since the in-source CID fully dissociates the hydrated uranium species at 386 m/z (Fig. S1), it was not monitored in this figure. As in the case of the in-source CID, and seen in Fig. S2, there are counteracting effects in setting the gas pressure. At low pressures, the extent of CID increases with pressure, while at higher values the overall throughput of Q2 decreases. In general, the desired analyte ions are far less affected by the increases in gas pressure than the corresponding signals of the background, with those species dropping more precipitously at 1.5 mTorr. This is observed to have a large effect on S/B for all analytes, although they do not all have a maximum at 1.5 mTorr. This is due to the larger collisional cross section of the background molecular species.[40] The 1.5 mTorr value was ultimately chosen as most acceptable based on the spectral quality observed for injections at low concentrations (250 ng mL^{-1}), where higher pressures yielded poor S/B characteristics.

Application of Different MS/MS scan modes

With the LS-APGD sampling by the TSQ optimized, the full benefits of a triple quadrupole instrument, the variety of MS/MS scan modes, were investigated to survey the types of fundamental information available to improve understanding of the processing occurring in the microplasma. Here again, this instrument differs substantially from those used in ICP-QqQ-MS where Q1 sets the entry masses into Q2

which is operated as a CRC, alleviating the presence of undesired secondary reaction products; the goal being better analytical accuracy. Here we wish to identify specific ion species and relate them to fundamental plasma processes. As a starting point for this set of illustrations, Fig. 3 shows a full scan from m/z = 10 to 400 Da of the 25 μg mL^{-1} multi-element (Rb, Ag, Tl, U) solution. From this spectrum, numerous species other than the main analyte signals are observed. While the analyte signals are more intense, there is a variety of background ions which can be generally attributed to water-related species. In addition, a number of the analytes also form oxides, hydrated species, salts and clusters. The value of having the full MS/MS experimental arsenal allows assignment of species, such as that labeled Ag_2X. In that case, it is easy to visually assign the identity as a Ag-dimer, but MS/MS is needed for correct identification. The various MS/MS modalities are demonstrated below for this primary test solution.

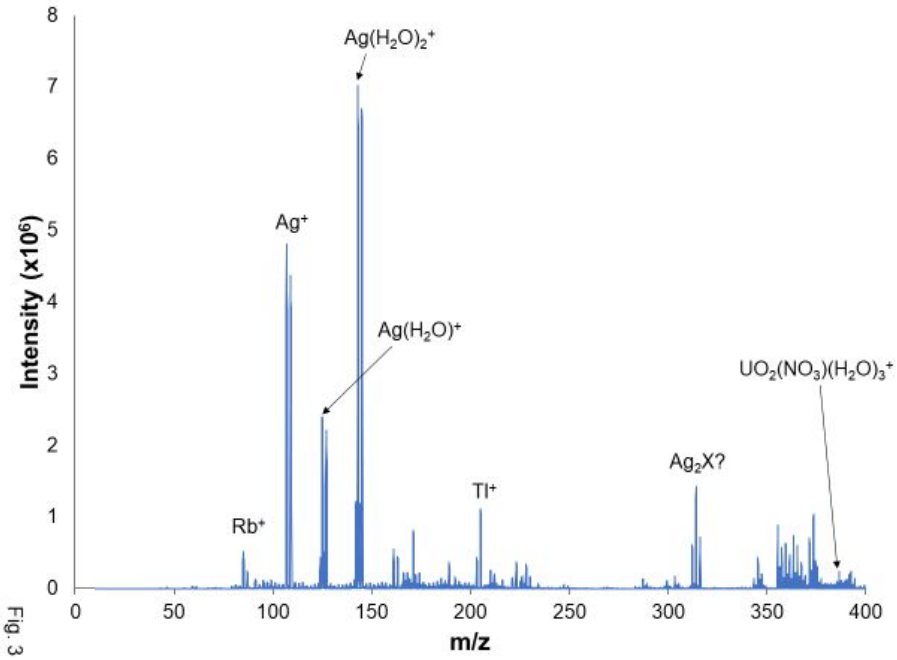

Figure 3. LS-APGD mass spectrum for a 25 μg mL^{-1} solution containing Rb, Ag, Tl, and U. The spectrum shown employs no collisional dissociation methods,

representing the native population of ions sampled into the mass spectrometer. Discharge conditions were those presented in Table 1.

To investigate what the various molecular species might be, parent ion, neutral loss, and product ion scanning modes were utilized. The main concepts of each scan are illustrated in Fig. 4. A quick parametric optimization was undertaken regarding the Q2 gas pressure and collisional energy for each of these scan types. In the first case, parent ion scans, the principle idea is to identify which of the ions produced in the plasma can be dissociated to the target analyte ions. In this mode, Q1 is scanned to successively higher masses, those ions are subjected to CID in Q2, and Q3 is held constant at the target ion m/z. Figure 5 is a comprehensive set of parent ion scans for the various analyte ions in the test mixture, reflecting the molecular ions that fragment to yield the identified analyte species. The spectral information can be quite enlightening.

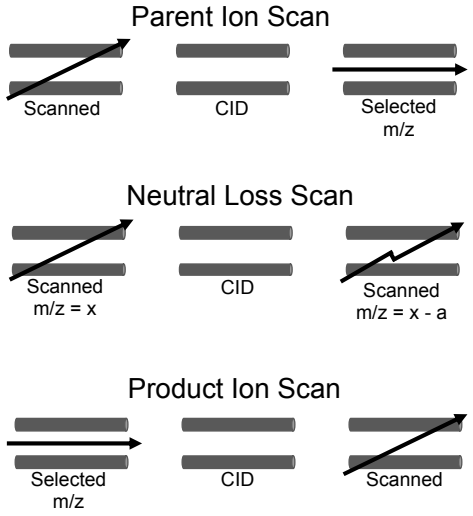

Fig. 4

Figure 4. Diagrammatic representation of the operating principles for the various MS/MS modes available in the LS-APGD/TSQ pairing. In each scan mode, Q2 is used for collisional dissociation, pressurizing the cell with Ar and applying an offset potential. Q1 is used to control what enters into Q2, while Q3 determines which masses reach the detector.

As a simple example, for the case of ^{205}Tl, the green-colored spectrum identifies the fact that Tl^+ is the primary ion entering Q1, while $Tl(H_2O)^+$ (m/z = 223 Da) makes up ~20% of Tl species, and $Tl(NOH)^+$ (m/z = 246 Da) is ~3% of the total thalium ion signal. While the monoatomic Tl^+ is the primary species for that element, the case is completely different for UO_2^+ where there is a plethora of higher mass species that dissociate to that ion.

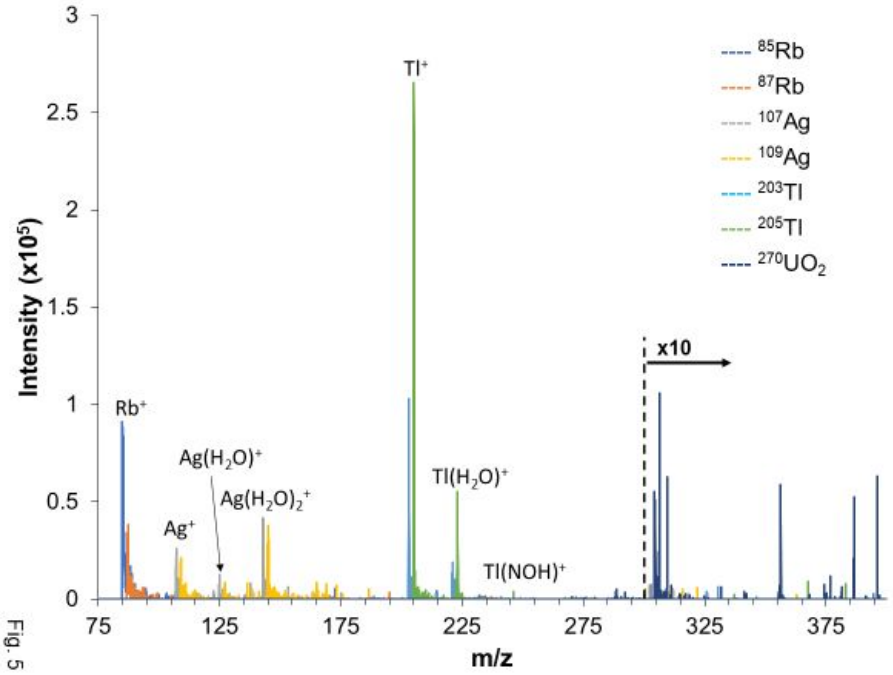

Figure 5. Parent ion scan performed for a 25 μg mL^{-1} solution containing Rb, Ag, Tl, and U. The entire mass range was allowed into Q2 for dissociation, while Q3 isolated each analyte isotope. All responses above m/z = 300 Da have been multiplied 10x. Discharge conditions were those presented in Table 1.

The evaluation of roles of the pole bias and target gas pressure was completed in the parent ion scan mode as a means of eventually generating the largest analyte ion signals (bare metal ions and UO_2^+). The extracted ion chromatograms (i.e., the integrated responses), integrated across all species producing the selected analyte masses in Q3 of each analyte isotope, were monitored under each set of CID

conditions. The maximum values in the chromatograms are expected to be the point in which optimum fragmentation occurs to yield the analyte species. Seen in Fig. S3a, a maximum yield with respect to the collision energy is found at 25 V for each of the analyte species. The response reflects greater levels of efficiency with increasing voltage, followed by ion losses (scattering) due to excess kinetic energies. In Fig. S3b, there is no clear, universal optimum in the Q2 gas pressure. Detailed interrogation across the individual spectra suggested that the greatest spectral clarity relative to the background water-related ions was obtained at a Q2 cell pressure of 1.5 mTorr Ar. Thus, a Q2 bias of 25 V and pressure of 1.5 mTorr Ar was used through the remainder of the studies. .

The neutral loss scan mode was utilized to identify the variety of water-related species formed within the plasma. This scan looks for any peaks that lose a mass of a specified value (e.g., 18 Da for H_2O) when collisional dissociation is applied, both Q1 and Q3 are set to scan ranges of the same width though they are offset by the user defined mass. For example, when identifying species that lose H_2O, Q1 may be set to scan from 50-200 m/z whereas Q3 is scanning from 32-182 m/z. Shown in Fig. 6, much of the spectra (from diverse neutral losses) are primarily made up of clusters of two or fewer water molecules. This mode was optimized in the same manner as the parent ion scan, monitoring the extracted ion chromatograms, with the optimum Q2 values yielding losses of those species being a pole bias of 25 V and a target gas pressure or 0.5 mTorr Ar determined (shown in Figs. S4 and S5). The preponderance of water related species is expected as the LS-APGD is a water-based plasma. It is important to note that when looking at the water species in Fig. 6, that the species present have

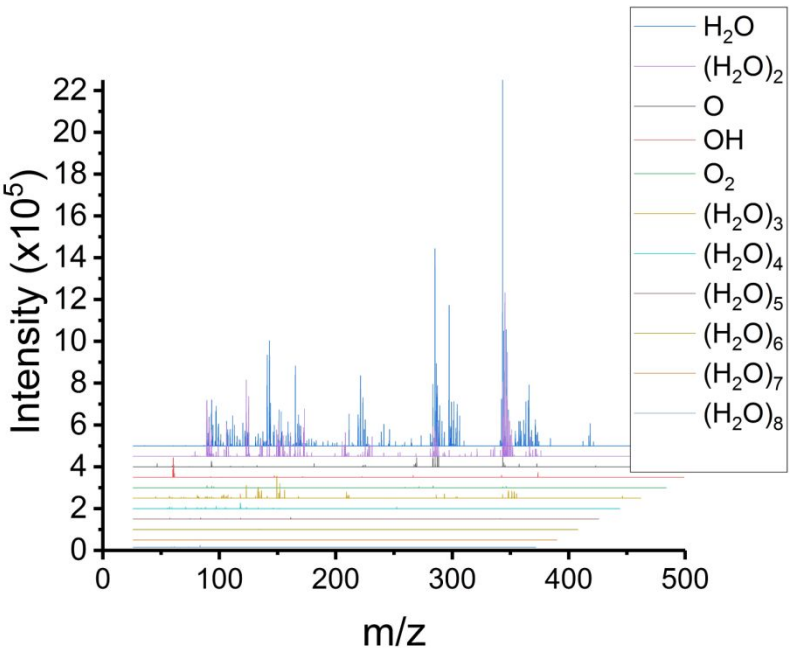

Fig. 6

Figure 6. Neutral loss spectra performed for a 25 μg mL^{-1} solution containing Rb, Ag, Tl, and U. The mass offset between Q1 and Q3 was to monitor the loss of oxide, hydroxide, and various water-cluster species. Discharge conditions were those presented in Table 1.

considerably lower intensities than the analyte species seen in Fig. 3 (though the spectra are taken with the same plasma conditions). Of course, the ions detected are charged species, with the vast majority carrying the charge of a single proton (H^+). Based on the scan format, Fig. 6 shows that the vast majority of species that lose water-related ions are themselves protonated water clusters. Indeed, the spectra suggest the presence of clusters that can lose up to 8 water molecules. Thus, very large water clusters are present. It should be noted that the same sort of scan would identify clusters containing remnants of the HNO_3 electrolyte in solution.

In addition to parent ion and neutral loss scans, product ion scans were also investigated. In this scan mode, Q1 is set to allow only a selected mass through, Q2 is used for fragmentation of the selected ion, and Q3 is set to scan over a defined range to

identify the product fragment ions. This is the more-or-less classic MS/MS mode used to identify organic species as a specific peak can be isolated and fragmented in order to determine its identity. As an example of the investigatory power of MS/MS for plasma diagnostics, Fig. 7 shows a product scan isolating masses 312, 314, and 316 which are identified in Fig. 3 as being related to a dimer of Ag. By fragmenting these peaks at the set conditions, the identity of parent ion can be inferred, with sufficient fragmentation to elucidate the complex' identity. The parent peak species are entirely fragmented by CID, with the loss of one water (loss of 18 from the parents) and two water molecules being the prominent products. Very little of the bare Ag metal ions are present under these CID conditions, which is not a surprise as the Ag-Ag bond energy is ~7 eV.[41] The low intensity products, though, confirm the existence of the dimer in the parent. Selective dissociation of the 312 Da parent yields entirely ^{107}Ag isotope signals, dissociation of 314 Da yields both ^{107}Ag and ^{109}Ag isotopes, and the 316 Da parent is composed entirely of the ^{109}Ag isotope; confirming that this is indeed a Ag dimer. With

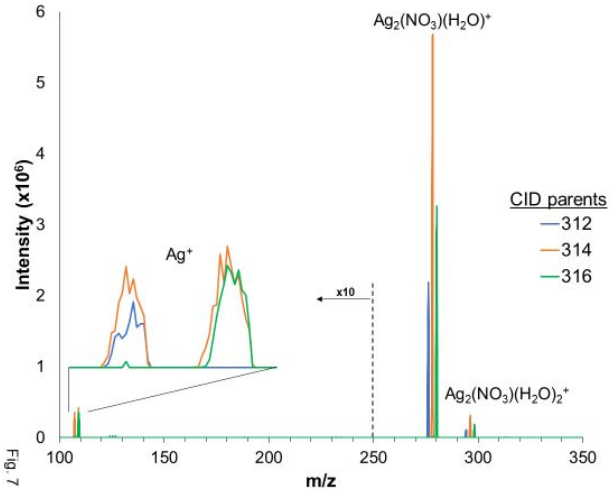

Figure 7. Product ion scan for the isotopes of the Ag dimer molecular species at m/z = 312, 314, and 316 Da obtained from a 25 μg mL^{-1} solution. Masses below 250 are multiplied 10x. Discharge conditions were those optimized in Table 1.

Ag_2 being the base unit and the isotope cluster centered at 276 Da representing the loss of two water molecules, means that the remaining mass difference can be attributed to a NO_3 unit, and so the complex can be identified as $Ag_2(NO_3)(H_2O)_2$. As shown here, this type of scan scenario can be extremely beneficial when trying to determine the identity of unknown species.

In addition to these directed-scan methods, the use of the collisional cell (Q2) for the generic removal of unwanted molecular species was investigated. CID was performed operating Q1 in an rf-only (band pass) mode, pressurizing the Q2 cell with argon and applying an offset potential in Q2, and operating Q3 in a mass-resolving mode. In this mode, the larger molecular ions will be expected to undergo an increased number of collisions, reducing the intensity through scattering and dissociation, while leaving the atomic species largely unchanged. To illustrate this simple strategy, a 25 μg mL^{-1} Pb solution was utilized as it forms a number of molecular species in the plasma. No in-source CID is applied in this instance so as to illustrate worst-case spectral features. By increasing the potential difference between Q1 and Q2 (i.e., the energy available for CID), an effective decrease in molecular species could be seen without affecting the intensity of the atomic Pb. In Fig. 8, the molecular Pb species, PbOH, $PbNO_3$, and $Pb(NO_3)(H_2O)$ can be seen as the most abundant species with no difference (0 V) between Q1 and Q2. As the potential difference is increased, up to a value of 29 V (the point at which spectral resolution began to be sacrificed), an almost complete reduction the molecular Pb species is seen, illustrating avenues for better-controlled background reductions than the in-source collisional method typically used.

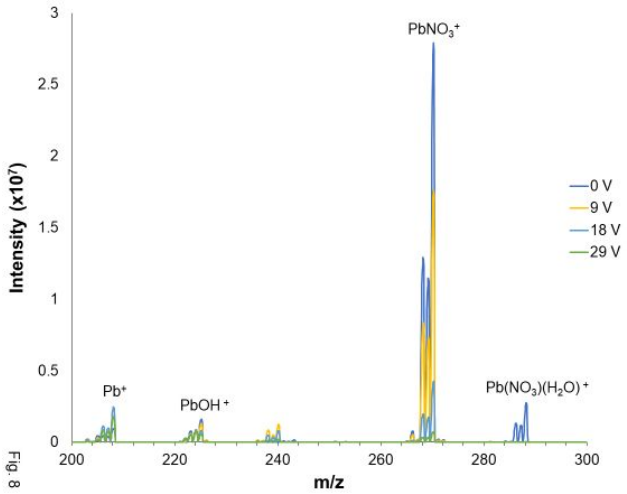

Figure 8. Effect of collisional induced dissociation in Q2 on the mass spectra from a 25 μg mL^{-1} Pb solution. Discharge conditions were those presented in Table 1.

The CID method of molecular species reduction is not implemented in commercial ICP-MS instruments, focusing instead on using reaction gases to chemically-separate interfering species or to permit the use of kinetic energy discrimination (KED).[42] Unfortunately, one limitation of the present triple-quadrupole platform is that there is not sufficient pumping capacity to allow Q2 pressurization with helium gas (as used in ICP-MS) nor can the relative Q2/Q3 offset potentials be varied under the system software.

Ultimately the breadth of information that can be obtained can be of great use. As shown above, the elemental species here form a variety of solvent related species. When introducing new species to the plasma, a parent ion scan simplifies the determination of what form the species is taking. Furthermore, this scan may prove useful for speciation studies. The neutral loss scan details a huge number of species formed from solvent adducts. Past works have detailed the formation and reduction of these solvent adducts based on plasma operating conditions, but this system could provide a much more powerful tool in determining the effects of plasma parameters. Lastly, the parent ion scan demonstrates an important capability in the determination of

unknown species forming within the plasma. While all of these methods have great benefits for elemental species, they will surely have enormous benefits when combined with the molecular sampling capabilities of the LS-APGD.

Preliminary Limits of Detection and Matrix Effects

Typically, ICP-OES/MS calibration curves are created using multielement standards, taking advantage of the capabilities of the devices. In an effort to assess the baseline sensitivity of the LS-APGD/TSQ coupling, the MS was operated at the optimized discharge conditions listed in Table 1 in a single quadrupole mode, where Q1 was the mass analyzer, utilizing Q2 and Q3 simply as ion guides. In-source CID and Q2 gas pressure were operated to 175 V and 1.5 mTorr, respectively. Triplicate 50 µL injections of the multielement solution used previously (250 ng mL^{-1} - 250 µg mL^{-1}) were performed monitoring the analyte responses at the most intense isotope for each. As the concentration exceeded 10 µg mL^{-1}, deviations from linearity occurred. As examples, Fig. 9 depicts the isotopic responses as a function of concentration. It can be seen that at 25 µg mL^{-1} of U as $^{238}UO_2^+$ (total metal concentration of 100 µg mL^{-1}), the response of U reaches a maximum and begins to decrease. Rb on the other hand appears to be preferentially ionized over U with a sharp increase intensity beginning at 25 µg mL^{-1}. A similar trend in signal suppression occurs with Ag and Tl although at higher concentrations (50 µg mL^{-1} of Ag and Tl each, with a total metal concentration of 200 µg mL^{-1}). As evidence of potential overloading of the plasma, a single-element U calibration curve was linear (R^2 = 0.9941) from 0.25 – 250 µg mL^{-1}, with severe

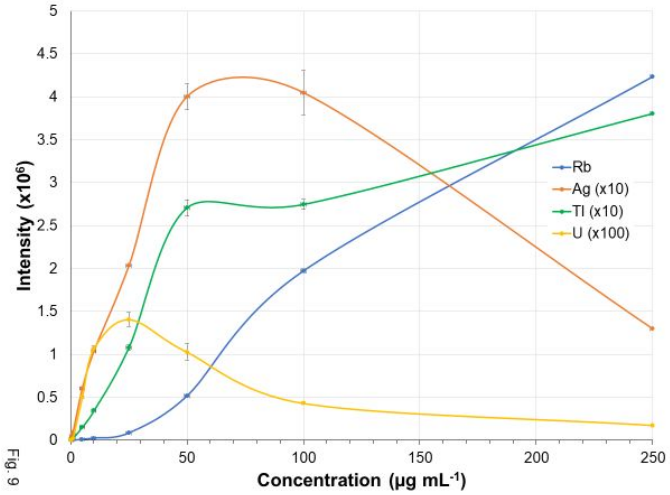

Figure 9. Effect of increasing total metal concentrations on analyte response for the multielement test solution. Discharge conditions were those presented in Table 1.

suppression in response beyond that point. This general set of signal suggests an overloading of the plasma, resulting in inefficient ionization of the higher ionization potential species; clearly a matrix effect that must be considered. That said, total solution concentrations of >100 μg mL^{-1} are above the typical concentration realm of plasma source MS. Certainly, sample dilution under such situations is feasible.

Due to the plasma mass overload effects, calibration curves for the multielement solution, Table 2, were restricted to less than 10 μg mL^{-1} for each of the four elements; a total loading of 40 μg mL^{-1}. Limits of detection were calculated using the following equation

$$LOD = \frac{3\sigma_B}{m}$$

where σ_B is the standard deviation of the blank and m is the slope of the calibration curve and 3 equals a 99% confidence interval. Presented in Table 2, the resulting LODs range from 0.99 to 38 ng mL^{-1} which are on par with those previously obtained on

the ThermoFisher LCQ Advantage.[30] More importantly for the cases of sample-limited or chromatographic analyses, these concentrations correspond to analyte mass values of 50 – 250 pg. Given the fact that the primary purpose of the interfacing of the LS-APGD microplasma to this triple-quadrople is for fundamental plasma diagnostics, it is felt that this level of sensitivity is more than sufficient for that effort.

Table 2: Calculated LODs for Rb, Ag, Tl, and U from calibration curves. Concentrations ranging from 250 ng mL^{-1} to 10 µg mL^{-1} were used.

Element	R^2	LOD (concentration)	LOD (absolute mass)
Rb	0.9939	0.99 ng mL^{-1}	50 pg
Ag	0.9936	4.9 ng mL^{-1}	250 pg
Tl	0.9963	38 ng mL^{-1}	2 ng
U	0.9954	3.5 ng mL^{-1}	180 pg

Conclusion

The LS-APGD microplasma has been interfaced to a triple-quadrupole platform (ThermoScientific TSQ) providing the capabilities to affect a comprehensive suite of MS/MS modalities. The primary objective was to yield an instrument that provides great flexibility to identify diverse plasma species and provide insights into fundamental processes. A simple multielement test solution (Rb, Ag, Tl, and U) provided a diversity of analyte-related molecular species. A thorough multi-parametric evaluation of the LS-APGD source operation conditions was performed in this first coupling to a triple quadrupole mass spectrometer. Beyond this, the in-source CID and Q2 gas pressures were optimized to reduce background species leading to significantly improved S/B ratios. In this new instrument coupling, multiple MS/MS scan modes have been

explored, illustrating the diversity of information that can be obtained. Parent ion scanning has been utilized to identify the various molecular species which might include the target analyte ions. In addition, neutral loss scanning was used to identify the presence of oxide, hydroxide, and water cluster species that make up the background spectra. Many of these species are formed via the clustering of water molecules or their addition to analyte ions. Some of these water-related species would have been unidentifiable in previous studies using trapping type instruments due to the limitations of MS/MS modalities. Finally, product ion scanning was employed to illustrate the ability to generically reduce molecular species relative to the target analyte ions. The sensitivity of the instrument was evaluated in a single-quadrupole mode, revealing a clear case of plasma overload above total analyte concentrations of ~100 mg mL^{-1} for 50 μL injections. LODs on the level of sub-to-single ng analyte mass are deemed sufficient for continued fundamental efforts.

Future work in this coupling will look into how plasma conditions, such as electrolyte compositions, affect the different analyte molecular species formed. A more in-depth analysis of the formation of background species will be performed as well. Ultimately, use of a comprehensive triple-quadrupole will permit the expansion of efforts in the use of the LS-APGD microplasma in the realms of organic[32] and organometallic[31] molecular mass spectrometry where MS/MS is essential in structural elucidation.

Conflicts of Interest

There are no conflicts of interest to declare.

Acknowledgements

This work was supported by the Defense Threat Reduction Agency, Basic Research Award #HDTRA1-14-1-0010, to Clemson University.

References

1. R. S. Houk, V. A. Fassel, G. D. Flesch, H. J. Svec, A. L. Gray and C. E. Taylor, *Anal. Chem.*, 1980, **52**, 2283-2289.

2. R. S. Houk, *Anal. Chem.*, 1986, **58**, 97A-105A.

3. S. D. Tanner, M. Paul, S. A. Beres and E. R. Denoyer, *At. Spectrosc.*, 1995, **16**, 16-18.

4. N. Jakubowski, L. Moens and F. Vanhaecke, *Spectrochim. Acta Part B-At. Spectrosc.*, 1998, **53**, 1739-1763.

5. D. C. Baxter, I. Rodushkin and E. Engstrom, *J. Anal. At. Spectrom.*, 2012, **27**, 1355-1381.

6. D. W. Koppenaal, C. J. Barinaga and M. R. Smith, *J. Anal. At. Spectrom.*, 1994, **9**, 1053-1058.

7. M. Iglesias, N. Gilon, E. Poussel and J. M. Mermet, *J. Anal. At. Spectrom.*, 2002, **17**, 1240-1247.

8. D. W. Koppenaal, G. C. Eiden and C. J. Barinaga, *J. Anal. At. Spectrom.*, 2004, **19**, 561-570.

9. J. W. Olesik and D. R. Jones, *J. Anal. At. Spectrom.*, 2006, **21**, 141-159.

10. N. Sugiyama and Y. Shikamori, *J. Anal. At. Spectrom.*, 2015, **30**, 2481-2487.

11. E. Bolea-Fernandez, L. Balcaen, M. Resano and F. Vanhaecke, *J Anal Atom Spectrom*, 2017, **32**, 1660-1679.

12. J. T. Rowan and R. S. Houk, *Appl. Spectrosc.*, 1989, **43**, 976-980.

13. K. L. Busch, G. L. Glish and S. A. McLuckey, *Mass Spectrometry/Mass Spectrometry: Techniques and Applicaitons of Tandem Mass Spectrometry*, VCH, New York. 1988.

14. S. A. McLuckey, *J. Am. Soc. Mass. Spectrom.*, 1992, **3**, 599-614.

15. R. C. A. Machado, C. D. B.; Schiavo, D.; Nobrega, J. A.; Nogueira, A. A., *Microchem. J.*, 2017, **130**, 271-275.

16. J. A. V. A. Barros, A. Virgilio, D. Schiavo and J. A. Nobrega, *Microchem. J.*, 2017, **133**, 567-571.

17. L. Fu, S. Y. Shi and X. Q. Chen, *Spectrochim. Acta, Part B - At. Spectrosc.*, 2017, **133**, 34-39.

18. R. Thomas, *Practical Guide to ICP-MS*, CRC Press, Boca Raton, Fl. 2013.

19. E. D. Hoegg, B. A. Patel, D. D. Richardson and R. K. Marcus, *J. Anal. At. Spectrom.*, 2018, **33**, 2015-2020.

20. P. Mezei and T. Cserfalvi, *Appl Spectrosc Rev*, 2007, **42**, 573-604.

21. Z. Z. Q. He and S. Hu, *Appl Spectrosc Rev*, 2013, **49**, 249-269.

22. P. Jamroz, K. Greda and P. Pohl, *TrAC- Tr. Anal. Chem.*, 2012, **41**, 105-121.

23. T. Cserfalvi and P. Mezei, *Fresen J Anal Chem*, 1996, **355**, 813-819.

24. T. Cserfalvi and P. Mezei, *J. Anal. At. Spectrom.*, 1994, **9**, 345-349.

25. T. Cserfalvi, P. Mezei and P. Apai, *J. Phys. D. Appl. Phys.*, 1993, **26**, 2184-2188.

26. M. R. Webb, G. C. Y. Chan, F. J. Andrade, G. Gamez and G. M. Hieftje, *J. Anal. At. Spectrom.*, 2006, **21**, 525-530.

27. R. K. Marcus, B. T. Manard and C. D. Quarles, *J. Anal. At. Spectrom.*, 2017, **32**, 704-716.

28. W. C. Davis and R. K. Marcus, *J. Anal. At. Spectrom.*, 2001, **16**, 931-937.

29. R. K. Marcus, C. D. Quarles, C. J. Barinaga, A. J. Carado and D. W. Koppenaal, *Anal. Chem.*, 2011, **83**, 2425-2429.

30. L. X. Zhang, B. T. Manard, S. Konegger-Kappel and R. K. Marcus, *Anal. Bioanal. Chem.*, 2014, **406**, 7741-7741.

31. L. X. Zhang, B. T. Manard, B. A. Powell and R. K. Marcus, *Anal. Chem.*, 2015, **87**, 7218-7225.

32. L. X. Zhang and R. K. Marcus, *J. Anal. At. Spectrom.*, 2016, **31**, 145-151.

33. E. D. Hoegg, R. K. Marcus, D. W. Koppenaal, J. Irvahn, G. J. Hager and G. L. Hart, *Rapid Commun Mass Sp*, 2017, **31**, 1534-1540. DOI: 10.1002/rcm.7937.

34. E. D. M. Hoegg, R. K.; Hager, G. J.; Hart, G. L.; Koppenaal, D. W., *J. Anal. At. Spectrom.*, 2018.

35. E. D. Hoegg, C. J. Barinaga, G. J. Hager, G. L. Hart, D. W. Koppenaal and R. K. Marcus, *J. Am. Soc. Mass. Spectrom.*, 2016, **27**, 1393-1403.

36. E. D. Hoegg, C. J. Barinaga, G. J. Hager, G. L. Hart, D. W. Koppenaal and R. K. Marcus, *J. Anal. At. Spectrom.*, 2016, **31**, 2355-2362.

37. C. D. Quarles, A. J. Carado, C. J. Barinaga, D. W. Koppenaal and R. K. Marcus, *Anal. Bioanal. Chem*, 2012, **402**, 261-268. DOI: 10.1007/s00216-011-5359-7.

38. E. D. Hoegg, B. A. Patel, W. N. Napoli, D. D. Richardson and R. K. Marcus, *J. Anal. At. Spectrom.*, 2018, **33**, 2015-2020.

39. M. C. A. Bevilacqua, and M. Sinigaglia, Formatex Research Center, Microbiology Book Series. 2010, vol. pp. 1419-1429.

40. N. I. Rousis, L. N. Pasias and N. S. Thomaidis, *Anal. Methods*, 2014, **6**, 5899-5908.

41. Q. S. Ran, R. W. Schmude, K. A. Gingerich, D. W. Wilhite and J. E. Kingcade, *J. Phys. Chem.*, 1993, **97**, 8535-8540.

42. N. Yamada, *Spectrochim. Acta, Part B - At. Spectrosc.*, 2015, **110**, 31-44.